DOI: 10.1021/ma1007144

Macromolecules
COMMUNICATION TO THE EDITOR

Acetylene Gas Mediated Conjugated Microporous Polymers (ACMPs): First Use of Acetylene Gas as a Building Unit

Jung Hoon Choi, Kyung Min Choi, Hyung Joon Jeon, Yoon Jeong Choi, Yeob Lee, and Jeung Ku Kang*

NanoCentury & EcoEnergy KAIST Institutes, Department of Materials Science & Engineering Korea Advanced Institute of Science and Technology, Daejeon 305-701, Republic of Korea

Received April 2, 2010
Revised Manuscript Received June 2, 2010

Although a significant progress has been achieved in the field to synthesize advanced microporous organic materials via linking organic building units into polymer networks, it still remains very difficult to fabricate the porous organic structures having the permanent microporosity due to the softness of organic molecules.[1] Meanwhile, Yaghi and co-workers have recently demonstrated that the synthesis of covalent organic frameworks (COFs)[2] having the microporosity is feasible by the condensation of boronic acid. In addition, recently a large number of microporous organic networks such as covalent triazine-based frameworks (CTFs)[3] and conjugated microporous polymers (CMPs)[4] have been also synthesized by linking the proper organic building units.

Microporous organic materials can provide the high surface areas, large pore volumes, and good chemical/thermal stabilities, thus having the great potentials for many applications including the storage for renewable hydrogen, the capture for carbon dioxide related to the greenhouse effects,[5] the removal of the dyes contaminated in water,[6] the heterogeneous catalysts for synthesis of chemicals,[7] and the photocatalysts for water splitting.[8] Despite these advantages, the conventional microporous materials generally do not have the functional groups allowing the modification into their versatile derivatives. In this view, it will be on a unique and novel approach if we could develop the microporous nanostructures linked with functional organic building units such as acetylene gas, which enables the modification after the synthesis, like organometallic complexes decoration[9] or metal cation-doped porous nanostructures[10] capable of being anchored on the functional organic linkers.

Among microporous organic materials, CMPs are of great interest because they have high surface areas and potential for organic electronics due to its conjugation. In general, CMPs with buildings unit having triple bond are synthesized by Sonogashira coupling reaction[11] connecting the alkyne monomer to the halogen monomer. In order to develop a cheap synthesis method allowable for the massive production of CMPs, it is necessary to reduce the synthesis process which is using two step-coupling reactions. Here, we report the facile method to synthesize microporous nanostructure so-called "acetylene mediated conjugated microporous polymers (ACMPs)" with functional linkers via the one-step Sonogashira reaction. In our approach, the iodine-terminated building units were directly linked by the triple bond of acetylene gas via one-step coupling reaction. Three types of ACMPs have been synthesized in this work. The starting building units and measured physical properties such as specific surface areas, pore volumes, and CO_2 adsorption capacities of ACMPs are summarized in Table 1. ACMP-C was fabricated by linking tetrakis(4-iodophenyl)methane with an acetylene gas, whereas ACMP-C6 and ACMP-N were synthesized from 1,3,5-tris(4-iodophenyl)benzene and tris(4-iodophenyl)amine, respectively.

The structures with the triple-bond linkages have been confirmed by the solid-state ^{13}C CPMAS NMR, as seen in Figure 1a where the chemical shift of a triple-bonded carbon corresponds to the peak at around 90 ppm. In addition, all of the carbon signals of the ACMPs were properly assigned with no residual carbon chemical shift. The ^{13}C CPMAS NMR spectra for the triple-bond linkage of the ACMPs were found to be consistent with those obtained from FT-IR measurements, where the C−C triple bond is giving the signal at 2200 cm^{-1} (Figure 1b).

The specific surface area, the pore volume, and the pore size determined using the N_2 isotherm at 77 K, as shown in Figure 2a. All ACMPs led to type I N_2 isotherms, indicating that the polymer networks have microporosity. The hysteresis of the isotherm is considered to be attributed to the swelling of the polymer networks in the condensed nitrogen.[12] The calculation of the Brunauer−Emmett−Teller (BET) surface area shows the values for 629 m^2/g for ACMP-C, 380 m^2/g for ACMP-C6, and 46 m^2/g for ACMP-N, as summarized in Table 1 with their Langmuir surface areas. ACMP-C gives the highest BET surface area. This is because the geometry of the starting material for ACMP-C has the tetrahedrally oriented iodine terminals suitable for formation of the microporous networks.

Meanwhile, ACMP-C6 was synthesized using a planar-type starting building unit with three iodine terminals less suitable for formation of 3-dimensional networked nanostructures compared to ACMP-C, as demonstrated by the smaller BET surface area of 308 m^2/g compared to that for ACMP-C. The starting building unit of ACMP-N is on the incomplete tetrahedron-type unit along with one lone pair electron, thus leading to a sparse network structure. This is expected to make the micropore network of ACMP-N very difficult to be accessed by N_2 molecules, and it resulted in the low BET surface area. It is noteworthy that NCMP-1[13] having the same polymer network structure as ACMP-N has been synthesized by the coupling reaction between alkyne monomer and halogen monomer, and it shows a relatively high BET surface area of 968 m^2/g. The surface area difference between ACMP-N and NCMP-1 suggests that the further study about optimization of reaction kinetics could lead to ACMPs having high surface areas. The total pore volumes calculated at $P/P_0 = 0.99$ for these three structures are also estimated to have 0.33 cm^3/g for ACMP-C, 0.31 cm^3/g for ACMP-C6, and 0.054 cm^3/g for ACMP-N. The pore size distribution of the ACMPs was calculated using Autosorb data-reduction software (version 1.55) from the N_2 isotherm using quenched solid density functional theory (QSDFT) with a N_2 slit pore kernel at 77 K. The pore size distributions of ACMPs are found to give 8.5 Å for ACMP-C, 9.3 Å for ACMP-C6, and 9.3 Å for ACMP-N (see Figure 2b). The amount of micropores showed a tendency proportional to their surface areas.

Figure 3a shows the molecular models for ACMPs generated using the Materials Studio 4.1 modeling package. All models were fully optimized using molecular dynamics simulation module with the COMPASS force field.[14] From the model calculation, we have found that the tetrahedral-type starting building unit of ACMP-C is feasible to make the cross-link with acetylene building unit, which leads to a high surface area. Meanwhile, in the case of ACMP-C6, the starting building unit is on the planar type,

*Corresponding author: Fax +82-42-350-3310; Tel +82-42-350-3338; e-mail jeungku@kaist.ac.kr.

 Published on Web 06/15/2010

Table 1. Reaction Scheme, Surface Areas, Pore Volumes, and CO_2 Adsorption Capacity of ACMPs

ACMPs [a]	Starting building unit (Halogen monomer)	Acetylene gas as a building unit	BET surface area	Langmuir surface area	Total pore volume [b]	CO_2 adsorption capacity [c]
ACMP-C			629 m^2/g	793 m^2/g	0.33 cc/g	503.4 mg/g
ACMP-C6	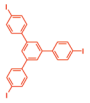		380 m^2/g	496 m^2/g	0.31 cc/g	438.9 mg/g
ACMP-N			46 m^2/g	61 m^2/g	0.054 cc/g	507.7 mg/g

[a] ACMPs were synthesized by coupling reaction between starting building unit (halogen monomer) and acetylene gas. [b] Total pore volumes were measured at 0.99 P/P_0. [c] The CO_2 isotherm was measured at 1.06 bar, 195 K.

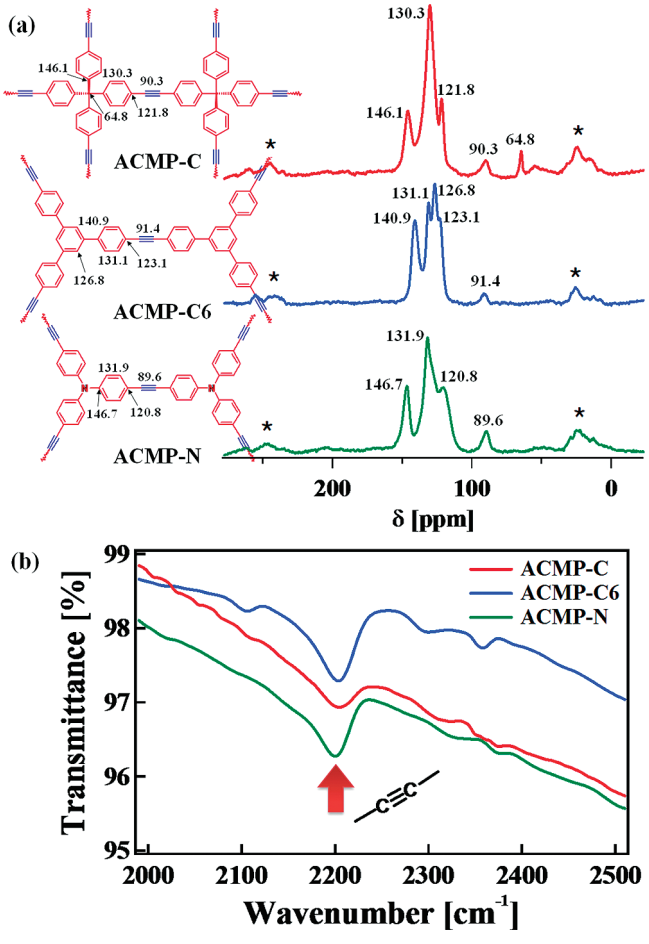

Figure 1. (a) Solid-state ^{13}C CPMAS NMR of ACMPs. The asterisk denotes the spinning sideband. (b) FT-IR spectrum of ACMPs.

so that the cross-linking is not high rather than that for ACMP-C, which explains a lower surface area of ACMP-C6 than that of ACMP-C. Furthermore, the starting building unit of ACMP-N is hard to make the cross-link because the bent starting building unit due to the lone pair electron of nitrogen atom do not offer the proper cross-linking angle. Therefore, ACMP-N leads to the lowest surface area because the low cross-linking results in a small amount of micropores. Parts b and c of Figure 3 show scanning electron microscope (SEM) images and high-resolution field emission transmission electron microscopy (FE-TEM) images of ACMPs, respectively. The SEM analysis shows that the morphologies of the ACMPs are based on the structures assembled by only the sphere phase with 10−100 nm scale sizes. A thermal-gravimetric analysis reveals that the ACMPs are stable up to 300 °C and that the maximum weight loss occurs at the temperatures above 500 °C. The ACMPs are stable in water and in general organic solvents such as chloroform, THF, acetone, methanol, hexane, and *N,N*-dimethylformamide.

Figure 4 shows the adsorption and desorption properties for CO_2 determined through the volumetric measurements at 195, 273, and 298 K. It is found that ACMP-C shows the highest CO_2 adsorption capacity among ACMPs. The CO_2 capacity of ACMP-C at 1.06 bar was 503.4 mg/g at 195 K, 68.8 mg/g at 273 K, and 47.5 mg/g at 298 K. Compared to one of metal−organic frameworks (IRMOF-1), ACMP-C shows the smaller CO_2 capacity at 195 K and 1 bar conditions by 3 times than 1489 mg/g[15] for IRMOF-1 having the large BET surface area of 3800 m^2/g. However, at 273 K, ACMP-C with the capacity of 68.8 mg/g at 1 bar showed the larger capacities compared to 66.1 mg/g[15] for IRMOF-1 and 59 mg/g[16] for the covalent organic framework (COF-5), having 1670 m^2/g BET surface area. Meanwhile, the CO_2 adsorption property of ACMP-N was 507.7 mg/g at 1.06 bar and 195 K, almost identical to the 503.4 mg/g for ACMP-C, despite the fact that the surface area of ACMP-N is ~13 times smaller than that of ACMP-C. The characteristics for adsorption of CO_2 on ACMP-N are considered to be attributed to the lone pair electrons of centered nitrogen atoms. These lone pair electrons would not be suitable for formation of the ideal network structure since they do not offer linking parts with other building units and the angle of the starting building unit differs slightly from a complete tetrahedral orientation. Meanwhile, the lone pair electrons appear to play an important role in that they can provide interaction sites through dipole−dipole interactions,[17] thus enhancing the carbon dioxide adsorption properties. For metal−organic frameworks (MOFs), to enhance the interaction between adsorbates and adsorbents, an open-metal site is commonly used.[18] We identify that the centered nitrogen of ACMP-N with the lone pair electron is playing the similar role to the open-metal site of MOFs. Another possible reason for the high CO_2 uptake of ACMP-N might be attributed to the smaller kinetic diameter for CO_2 of 3.3 Å than that for N_2 of 3.64 Å,[19] such that CO_2 molecules could access smaller pores which N_2 molecules are so difficult to access. Meanwhile, to give the more clear clarification, the Connolly surface areas along with the pore volumes[20] were calculated (see Supporting Information for the method, surface areas and pore volumes), and calculated

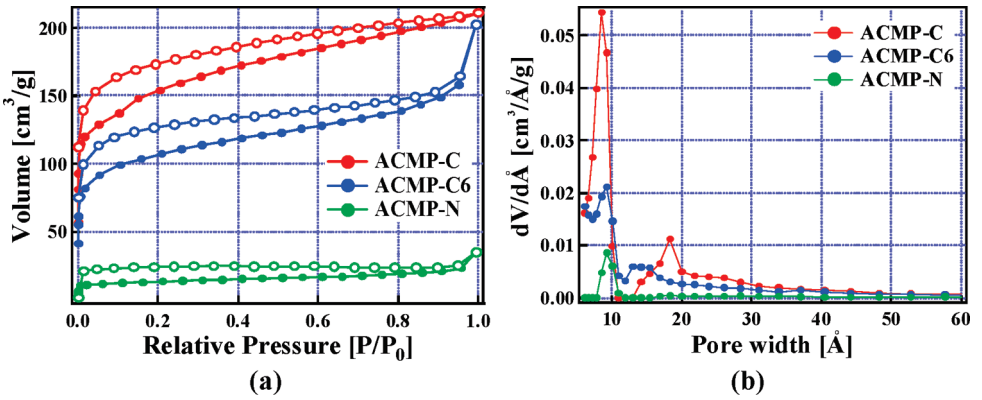

Figure 2. (a) N_2 adsorption (filled symbol) and desorption (open symbol) isotherms of ACMPs. (b) Pore size distributions of ACMPs calculated by the QSDFT method.

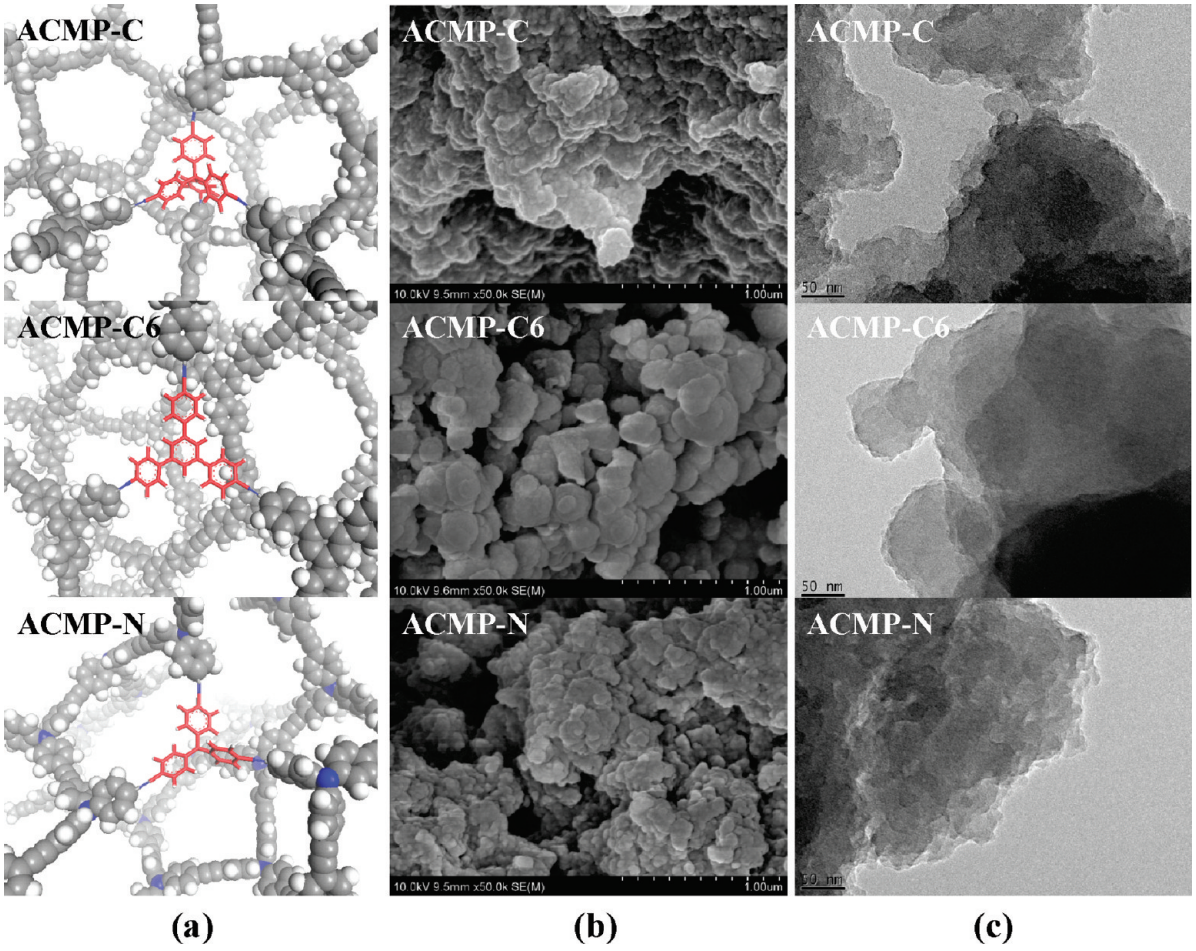

Figure 3. (a) Amorphous molecular models for ACMPs. C, N, and H are shown in gray, blue, and white, respectively. Repeating unit is emphasized as stick model (blue for triple bond and red for other bondings). (b) SEM images of ACMPs; scale bars are on the insets. (c) FE-TEM images of ACMPs; the scale bars are on the insets.

surface areas are 5242 m^2/g for ACMP-C, 2551 m^2/g for ACMP-C6, and 5635 m^2/g for ACMP-N, where the kinetic radius for nitrogen of 1.82 Å was used on the periodic modeling structures of ACMP-C, ACMP-C6, and ACMP-N. These are consistent with our experimental data in that the surface area for ACMP-C is almost twice larger than that for ACMP-C6. However, the calculated surface area of ACMP-N is similar to that for ACMP-C. In this view, we consider that the collapse of micropores in ACMP-N having a sparse network structure (Figure S4) resulted in the decreased pore diameter of ACMP-N and gave a small surface area from the experiment because N_2 cannot penetrate the pores while the small kinetic diameter of CO_2 could access to ACMP-N. Also, when the temperature increases from 195 to 273 and 298 K, the CO_2 uptake of ACMP-N decreases compared to ACMP-C, as seen in Figure 4b,c. This demonstrates that the increased kinetic diameter of CO_2 at high temperature prevents penetrating into the pores of ACMP-N, although it has lone pair electrons on nitrogen atom for a good interaction site with CO_2.

In conclusion, the facile method to synthesize "acetylene mediated conjugated microporous polymers (ACMPs)" with the functional linker of a triple bond have been developed for the first time via the one-step Sonogashira coupling between the acetylene gas

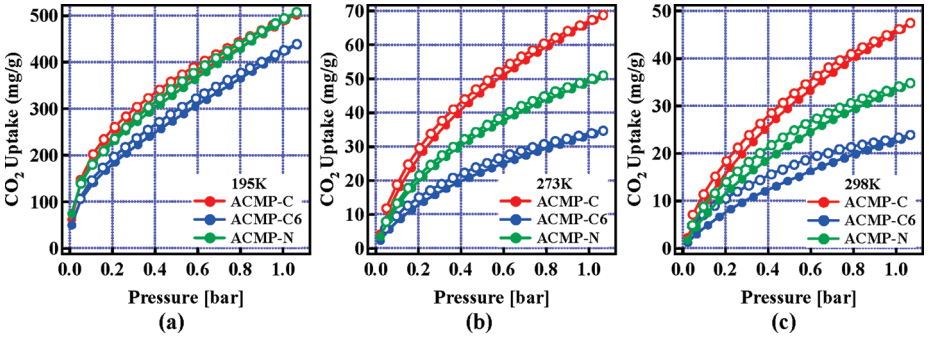

Figure 4. CO_2 adsorption and desorption property of ACMPs at (a) 195, (b) 273, and (c) 298 K.

and the halogen starting building units. In the formation of polymer networks or organic microporous materials, the acetylene gas was used as a building unit. The direct method using acetylene gas as a building unit is on a unique approach to form polymer networks, in that the conventional two-step reactions to synthesize CMPs have been reduced to the one-step coupling reaction. We also expect that this facile process could be further applied to synthesize various types of CMPs on a combination of the functional triple bond from acetylene gas with the halogen monomers. In addition, it was identified that the significant CO_2 uptake capacity of ACMP-N at 195 K are available due to the micropore network accessible by CO_2 with the small kinetic diameter, although the micropore network for ACMP-N was very difficult to be accessed by the N_2 molecules with a relatively large kinetic diameter. Meanwhile, as the temperature increases, we found that ACMP-C shows the highest CO_2 adsorption capacity among ACMPs with 68.8 mg/g at 273 K and 47.5 mg/g at 298 K. This demonstrates that the increased kinetic diameter of CO_2 at high temperatures prevents penetrating into the pores of ACMP-N, although it has lone pair electrons on nitrogen atom for a good interaction site with CO_2. ACMP-C shows the smaller CO_2 capacity by 3 times than 1489 mg/g for IRMOF-1 having the large BET surface area of 3800 m^2/g at 195 K. However, at 273 K, it was also found that ACMP-C showed the larger capacity compared to the 66.1 mg/g for IRMOF-1 and CO_2 capacity of 59 mg/g for the covalent organic framework (COF-5) having 1670 m^2/g BET surface area. Consequently, these results imply that the selective design of the starting building monomer could be very useful to realize the advanced gas storage materials.

Acknowledgment. This work was mainly supported by the Korea Center for Artificial Photosynthesis (KCAP) funded by the Ministry of Education, Science and Technology (NRF-2009-C1AAA001-2009-0093879), by the Hydrogen Energy R&D Center from one of the 21st Century Frontier R&D Program, and by the WCU (World Class University) program (R-31-2008-000-10055-0). Dr. Y. J. Choi's reseach fellowship was supported by the Priority Research Centers Program (NRF-2009-0094041). Also, J. H. Choi and K. M. Choi were supported in parts by the grants from National Research Foundation (NRF-R0A-2007-000-20029-0) and the Center for Inorganic Photovoltaic materials (NRF-2010-0007692).

Supporting Information Available: Details of the synthesis procedures, solid state NMR, FT-IR spectra, SEM and TEM analysis, gas sorption analysis, thermal gravimetric analysis, and specific surfaces area and pore volumes calculations. This material is available free of charge via the Internet at http://pubs.acs.org.

References and Notes

(1) Weber, J.; Antonietti, M.; Thomas, A. *Macromolecules* **2007**, *40*, 1299.
(2) (a) Côté, A. P.; Benin, A.; Ockwig, N.; Matzger, A.; O'Keeffe, M.; Yaghi, O. M. *Science* **2005**, *310*, 1166. (b) El-Kaderi, H. M.; Hunt, J. R.; Mendoza-Cortés, J. L.; Côté, A. P.; Taylor, R. E.; O'Keeffe, M.; Yaghi, O. M. *Science* **2007**, *316*, 268. (c) Uribe-Romo, F. J.; Hunt, J. R.; Furukawa, H.; Klöck, C.; O'Keeffe, M.; Yaghi, O. M. *J. Am. Chem. Soc.* **2009**, *131*, 4570.
(3) Kuhn, P.; Antonietti, M.; Thomas, A. *Angew. Chem., Int. Ed.* **2008**, *47*, 1.
(4) (a) Jiang, J.; Su, F.; Trewin, A.; Wood, C. D.; Campbell, N. L.; Niu, H.; Dickinson, C.; Ganin, A. Y.; Rosseinsky, M. J.; Khimyak, Y. J.; Cooper, A. I. *Angew. Chem., Int. Ed.* **2007**, *46*, 8574. (b) Jiang, J.-X.; Su, F.; Trewin, A.; Wood, C. D.; Niu, H.; Jones, J. T. A.; Khimyak, Y. Z.; Cooper, A. I. *J. Am. Chem. Soc.* **2008**, *130*, 7710. (c) Stöckel, E.; Wu, X.; Trewin, A.; Wood, C. D.; Clowes, R.; Campbell, N. L.; Jones, J. T. A.; Khimyak, Y. Z.; Adams, D. J.; Cooper, A. I. *Chem. Commun.* **2009**, *2*, 212. (d) Jiang, J-X.; Su, F.; Niu, H.; Wood, C. D.; Campbell, N. L.; Khimyak, Y. Z.; Cooper, A. I. *Chem. Commun.* **2008**, *4*, 486. (e) Cooper, A. I. *Adv. Mater.* **2009**, *21*, 1291.
(5) Furukawa, H.; Yaghi, O. M. *J. Am. Chem. Soc.* **2009**, *131*, 8875.
(6) Kuhn, P.; Krüger, K.; Thomas, A.; Antonietti, M. *Chem. Commun.* **2008**, *44*, 5815.
(7) Zhang, Y.; Riduan, S. N.; Ying, J. Y. *Chem.—Eur. J.* **2009**, *15*, 1077.
(8) Wang, X.; Maeda, K.; Thomas, A.; Takanabe, K.; Xin, G.; Carlsson, J. M.; Domen, K.; Antonietti, M. *Nature Mater.* **2009**, *8*, 76.
(9) Constable, E. C.; Gusmeroli, E.; Housecroft, C. E.; Neuburger, M.; Schaffner, S. *Polyhedron* **2006**, *25*, 421.
(10) Choi, Y. J.; Lee, J. W.; Choi, J. H.; Kang, J. K. *Appl. Phys. Lett.* **2008**, *92*, 173102.
(11) Sonogashira, K.; Tohda, Y.; Hagihara, N. *Tetrahedron Lett.* **1975**, *16*, 4467.
(12) McKeown, N. B.; Budd, P. M.; Msayib, K. J.; Ghanem, B. S.; Kingston, H. J.; Tattershall, C. E.; Makhseed, S.; Reynolds, K. J.; Fritsch, D. *Chem.—Eur. J.* **2005**, *11*, 2610.
(13) Jiang, J.-X.; Trewin, A.; Su, F.; Wood, C. D.; Niu, H.; Jones, J. T. A.; Khimyak, Y. Z.; Cooper, A. I. *Macromolecules* **2009**, *42*, 2658.
(14) Sun, H. *J. Phys. Chem. B* **1998**, *102*, 7338.
(15) Walton, K. S.; Millward, A. R.; Dubbeldam, D.; Frost, H.; Low, J. J.; Yaghi, O. M.; Snurr, R. Q. *J. Am. Chem. Soc.* **2008**, *130*, 406.
(16) Furukawa, H.; Yaghi, O. M. *J. Am. Chem. Soc.* **2009**, *131*, 8875.
(17) Millward, A. R.; Yaghi, O. M. *J. Am. Chem. Soc.* **2005**, *127*, 17998.
(18) Panella, B.; Hirscher, M.; Pütter, H.; Müller, U. *Adv. Funct. Mater.* **2006**, *16*, 520.
(19) Dybtsev, D. N.; Chun, H.; Yoon, S. H.; Kim, D.; Kim, K. *J. Am. Chem. Soc.* **2004**, *126*, 32.
(20) Connolly, M. L. *Science* **1983**, *221*, 709.